Measurement of finite frequency noise cross-correlations with a resonant circuit

Marjorie Creux, Adeline Crépieux, Thierry Martin

Measurement of finite frequency cross-correlations noise with a resonant circuit

M. Creux, A. Crépieux, and T. Martin

Centre de Physique Théorique, Case 907 Luminy,

13288 Marseille cedex 9, France and

Université de la Méditerranée, 13288 Marseille cedex 9, France

(Dated: May 12, 2006)

Abstract

The measurement of finite frequency cross-correlations noise represents an experimental challenge in mesoscopic physics. Here we propose a generalisation of the resonant LC circuit setup of Lesovik and Loosen which allow to probe directly such cross-correlations by measuring the charge fluctuations on the plates of a capacitor. The measuring circuit collects noise contributions at the resonant frequency of the LC circuit. Auto-correlation noise can be canceled out by switching the wires and making two distinct measurements. The measured cross-correlations then depend on four non-symmetrized correlators. This detection method is applied to a normal metal three terminal device. We subsequently discuss to what extent the measurement circuit can detect electron-antibunching and what singularities appear in the spectral density of cross-correlations noise.

PACS numbers:

I. INTRODUCTION

The measurement of finite frequency noise in mesoscopic systems provides a useful diagnosis of quantum transport: it allows to characterize the carriers which are involved. In normal metal conductors[1, 2], at zero temperature (and in the absence of spatial averaging effects [3, 4]), finite frequency correlations exhibit a singularity at $\omega = eV$. In normal metal-superconductor junctions [5], Andreev reflection gives rise to a singularity at $2eV$ signaling that Cooper pairs enter the superconductor, in the fractional quantum Hall effect, the tunneling of quasiparticles in the vicinity of a point contact leads to a singularity at $e\nu V$, with ν the filling factor[6]. At the same time, "zero" frequency noise cross correlations can be used to probe directly the statistics of the charge carriers: are the carriers bunched or anti-bunched[7]? This implies a "Y" geometry where carriers are injected in one arm, and correlations are measured in the two receiving arms. The purpose of the present work is to discuss an inductive coupling setup which can be used toward the measurement of high frequency noise correlations in such geometries.

Any setup for measuring noise involves the selection (filtering) of a range of specific frequencies by the electronic detection circuit. Provided that the electrical apparatus in an experiment can sample the current at discrete times, finite frequency noise can in principle be computed directly from this time series. Yet, a noise correlator is a quantum mechanical average of products of operators. Symmetrized or non-symmetrized correlators can thus be constructed from the time series, provided that the frequency is much smaller than the inverse time step of the series. This recipe for computing the noise is not practical at high frequencies. Here, we are interested in systems where noise is detected via a measuring device – coupled to the mesoscopic device which should pick up the noise contribution at a specific frequency, via repeated measurements. Such proposals have been put forth and some have been implemented experimentally within the last decade. Ref. [8] uses effectively a LC circuit in order to measure the noise of a two terminal diffusive conductor. A theoretical suggestion due to Lesovik and Loosen[9] consists of a LC circuit coupled inductively to the fluctuating current emanating from a mesoscopic conductor: the measurement of the charge fluctuations on the capacitor plates provides information on the finite frequency noise correlators at the resonant frequency of the LC circuit. The fact that this method samples contributions from the non-symmetrized noise correlators, which are related to emission and absorption from the device, has been emphasized in Ref. [10].

Aguado and Kouvenhoven[11] have proposed to measure the noise of an arbitrary circuit by coupling capacitively this circuit to a detector circuit: a DC current – generated by inelastic electron tunneling events – flows in the detector circuit when a "photon" $\hbar\omega$, is provided/absorbed by the mesoscopic circuit. This theoretical suggestion has been successfully implemented to measure the finite frequency noise of a Josephson junction using a large Superconductor-Insulator-Superconductor junction[12]: quasiparticles tunnelling in the SIS junction can occur only if it is assisted by the frequency provided by the antenna. A subsequent experiment allowed to isolate the emission and absorption contributions to noise [13]. High frequency noise measurements have been also performed using the detection of photons emitted by the mesoscopic conductor [14]. Such photons propagate in coaxial lines and are analyzed/detected in a Hanbury–Brown and Twiss geometry for microwave photons appeared in order to measure two terminal noise with an auxiliary mesoscopic circuit. Turning to noise cross correlations, low frequency noise measurement in such branched circuits have been performed[15], which showed that a fully degenerate electron gas has negative noise correlations. Cross-correlations noise have obvious applications in the study of electron transport in Hanbury–Brown and Twiss type geometries. Below, we will mention two situations where they are useful: the study of electronic entanglement in mesoscopic devices [16, 17], and the identification of anomalous charges in Luttinger liquid wires[18]. Here we consider the case of a setup where the cross-correlations noise are analyzed via inductive coupling to the mesoscopic circuit to be measured.

The paper is organized as follows. In section II, the model with a measuring circuit is introduced, and it is shown how cross-correlations can be directly obtained. In section III, we compute the measured cross-correlations noise. In section IV, we introduce a model with two separated circuits and we compute the measured cross-correlations noise. Our results, in the case of one circuit, are then applied in section V to a simple device: a three terminals normal metallic sample, where we stress the difference between the symmetrized noise, the non-symmetrized noise, and the measured noise. Section VI gives two examples where cross-correlations are needed. We conclude in section VII.

II. MODEL AND METHOD

For measuring cross-correlations, two inductances (L_1 and L_2) and a single capacitor (C) are needed. The two inductors having coupling constants α_1 and α_2, are placed next

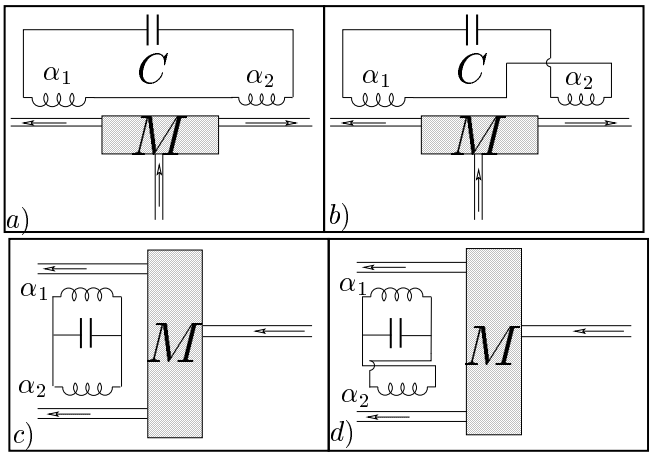

FIG. 1: Schematic description of the noise cross-correlation setup. M is the mesoscopic circuit to be measured, C is the capacitor and there are two inductors with coupling constants α_1 and α_2 to the mesoscopic circuit. a) and b): the electrical components of the detector are in series and they "see" the current with the same sign (a) or with the opposite sign (b). c) and d): the electrical components of the detector are in parallels and they "see" the current with the same sign (c) or with the opposite sign (d).

to the two outgoing arms of the three terminal mesoscopic device (Fig. 1). We consider two cases: the two inductances are placed in series (Fig. 1a and Fig. 1b) or in parallel (Fig. 1c and Fig. 1d). Depending on the wiring of these inductances (Fig. 1a,c or Fig. 1b,d), the two inductances "see" the outgoing currents with the opposite sign or with the same sign. Throughout this paper, we neglect the mutual inductance of the detector circuit: it is justified by the fact that such inductances are placed near opposite ends of the circuit whose noise correlations are measured. Classically, the charge x on the capacitor plates of the measuring circuit obeys the equation of motion:

$$M\ddot{x}(t) = -Dx(t) - \alpha_1 \dot{I}_1(t) \mp \alpha_2 \dot{I}_2(t) \ , \tag{2.1}$$

where the "mass" $M = L_1 + L_2$ if the circuit is in series (Fig. 1a,b) or $M = L_1 L_2/(L_1 + L_2)$ if the circuit is in parallel (Fig. 1c,d), and $D = 1/C$. The characteristic frequency of the LC circuit is $\Omega = \sqrt{D/M}$.

The currents which appear in the two coupling terms are $I_{1(2)}(t) = l^{-1} \int_{x_{1(2)}-l/2}^{x_{1(2)}+l/2} I(r,t)dr$, where l is the length of the inductive coupling region. We assume in a standard way that the chemical potential of the leads is the largest energy scale, compared to the bias voltage and the frequency we want to probe. Spatial averaging effects for the currents have been discussed

in Ref. [19, 20]: the current operator contains fast and slow oscillations [21], at least in the ballistic case. Here we claim to be measuring a current which is spatially independent because of the integral over the inductive region l. We first assume that $l \gg \lambda_F$, so that short wave lengths oscillations are averaged out. Furthermore, the slowly oscillating terms in the current will be reduced to a constant contribution if we require that $l \ll v_F/\omega$. Ref. [3] has studied the spatial oscillations of the current in the presence of Coulomb interactions: interactions modify the wavelength $\pi v_F/\omega$ of such oscillations, but the amplitude of its signal is reduced with increasing interaction strength.

The derivation of Ref. 9 is generalized to the two inductances situation. To quantize the measuring circuit, we note that the equation of motion can be derived from the Hamiltonian:

$$H = H_0 + H_{int} = \frac{p^2}{2M} + \frac{Dx^2}{2} + H_{int} \ , \tag{2.2}$$

with

$$H_{int} = -\frac{p(\alpha_1 I_1(t) \pm \alpha_2 I_2(t))}{M} + \frac{(\alpha_1 I_1(t) \pm \alpha_2 I_2(t))^2}{2M} \ . \tag{2.3}$$

The mesoscopic circuit plus measuring circuit are assumed to be decoupled at $t = -\infty$. The coupling between the two is switched on adiabatically, and one can monitor the charge of the capacitor, and its fluctuations, in the presence of the fluctuating currents at time $t = 0$: it is a stationary measurement.

The n-th power of the capacitor charge reads, in the interaction representation:

$$\langle x^n(0) \rangle = Tr[e^{-\beta H_0} U^{-1}(0) x^n(0) U(0)] \ , \tag{2.4}$$

with the evolution operator

$$U(0) = T \exp\left(\frac{-i}{\hbar} \int_{-\infty}^{0} dt' H_{int}(t')\right) \ . \tag{2.5}$$

We calculate perturbatively the n-th power of the charge, expanding the evolution term $(U(0))$ in powers of H_{int}. Considering the average charge and the average charge square, one obtains:

$$\langle x(0) \rangle \ = \ \langle x(0) \rangle_1 + \langle x(0) \rangle_3 + ... \ , \tag{2.6}$$

$$\langle x^2(0) \rangle \ = \ \langle x^2(0) \rangle_0 + \langle x^2(0) \rangle_2 + ... \ , \tag{2.7}$$

where the different orders in H_{int} are linked to the higher cumulants of the current: $\langle x(0) \rangle_1$ contains information about the average current, $\langle x^2(0) \rangle_2$ about the current fluctuations, and $\langle x(0) \rangle_3$ about the third moment, and so on.

The zero order contribution of the charge fluctuations gives:

$$\langle x^2(0)\rangle_0 = \frac{\hbar}{2M\Omega}(N(\Omega)+1/2)\ , \tag{2.8}$$

with $N(\Omega) = 1/(e^{\beta\hbar\Omega}+1)$ is the Bose Einstein distribution at the detector circuit temperature, which is not necessarily the mesoscopic device temperature. The next non-vanishing term, which depends on products of current operators is:

$$\begin{aligned}\langle x^2(0)\rangle_{2\pm} = \quad & \Big\langle \frac{1}{2M}\Big(\frac{-i}{\hbar}\Big)^2 \int_{-\infty}^{0} dt_1 \int_{-\infty}^{t_1} dt_2 \\ & \times\ [[x(0), p(t_1)(\alpha_1 I_1(t_1) \pm \alpha_2 I_2(t_1))], \\ & \quad p(t_2)(\alpha_1 I_1(t_2) \pm \alpha_2 I_2(t_2))]\Big\rangle \\ & -\ \frac{1}{2M}\Big(\frac{-i}{\hbar}\Big)\int_{-\infty}^{0} dt \langle I^2(t)\rangle\langle x^2(0)\rangle - \langle x^2(0)\rangle\langle I^2(t)\rangle\ ,\end{aligned} \tag{2.9}$$

where one recalls that the sign in front of the coupling constants $\alpha_{1,2}$ reflect the choice of the circuit, (a or b) and (c or d). The calculation of the charge fluctuations gives four terms: two autocorrelation terms which correspond to the fluctuations due to a single inductor (in terms of α_1^2 or α_2^2), and two terms associated with the correlation between the two inductors, which are proportional to $\alpha_1\alpha_2$. It is precisely these latter terms which allow to detect the noise correlations. Thus, it seems that it is impossible in practice to get rid of the autocorrelation terms: the measurement of the cross terms would require a prior knowledge of the charge fluctuations for a single impedance with a high degree of accuracy. We argue that this is not the case, provided that two measurements with the same setup but with different wiring can be achieved. One measures the charge fluctuations $\langle x^2(0)\rangle_{2+}$ with the geometry of Fig. 1a for the inductances in series (Fig. 1c for the parallel case), and subsequently one can switch the wiring and measure such fluctuations $\langle x^2(0)\rangle_{2-}$ with the circuit of Fig. 1b (Fig. 1d). In each case (series or parallel setup) by subtracting the two signals:

$$\langle x^2(0)\rangle_2 = \frac{1}{2}\big(\langle x^2(0)\rangle_{2+} - \langle x^2(0)\rangle_{2-}\big)\ , \tag{2.10}$$

one isolates the contribution of cross-correlations, which is proportional to $\alpha_1\alpha_2$. This combination of charge fluctuations, which in turn depends on current cross-correlators, will be referred from now on as the measured cross correlations.

III. MEASURED CROSS-CORRELATIONS AND NON-SYMMETRIZED NOISE

In order to proceed, the charge and the momentum are now written in terms of the oscillator variables of the LC circuit:

$$x(t) = \sqrt{\frac{\hbar}{2M\Omega}}(ae^{-i\Omega t} + a^\dagger e^{i\Omega t}) \ , \tag{3.1}$$

$$p(t) = i\sqrt{\frac{\hbar M\Omega}{2}}(a^\dagger e^{i\Omega t} - ae^{-i\Omega t}) \ , \tag{3.2}$$

where a is the destruction operator which satisfies $\langle a^\dagger a\rangle = N(\Omega)$. The first commutator in Eq. (2.9) becomes:

$$[x^2(0), p(t_1)I_i(t_1)] = \frac{2i\hbar}{M\Omega}\Big(\frac{\hbar M\Omega}{2}\Big)^{1/2}\cos(\Omega t_1)(a + a^\dagger)I_i(t_1) \ , \tag{3.3}$$

and the average of the two interlocked correlators of Eq. (2.9) reads:

$$\begin{aligned}\Big\langle\Big[[x^2(0), p(t_1)I_i(t_1)], p(t_2)I_j(t_2)\Big]\Big\rangle &= -\hbar^2\cos(\Omega t_1)\\ \times\ \Big\{&\langle I_i(t_1)I_j(t_2)\rangle\big[(N(\Omega)+1)e^{i\Omega t_2} - N(\Omega)e^{-i\Omega t_2}\big]\\ &-\langle I_j(t_2)I_i(t_1)\rangle\big[N(\Omega)e^{i\Omega t_2} - (N(\Omega)+1)e^{-i\Omega t_2}\big]\Big\} \ ,\end{aligned} \tag{3.4}$$

with $i, j = 1, 2$ $(i \neq j)$. Substituting this commutator in the expression of charge fluctuations, four correlators of current derivatives appear in the result. Translationnal invariance motivates the change of variables: $\{t_1, t_2\} \rightarrow \{t = t_1 - t_2, T = t_1 + t_2\}$. The charge fluctuations become:

$$\begin{aligned}\langle x^2(0)\rangle = \frac{\alpha_1\alpha_2}{(4M)^2}&\int_{-\infty}^{+\infty} dt \int_{-\infty}^{0} dT e^{\eta T}\\ \times\ \Big\{&(e^{i\Omega t} + e^{-i\Omega T sign(t)})\\ &\times[(N(\Omega)+1)(\langle I_2(0)I_1(t)\rangle + \langle I_1(0)I_2(t)\rangle)\\ &-N(\Omega)(\langle I_1(t)I_2(0)\rangle + \langle I_2(t)I_1(0)\rangle)]\Big\} \ .\end{aligned} \tag{3.5}$$

In a manner similar to Refs. 9 and 10, the following non-symmetrized current correlators are introduced in Fourier space:

$$S_{ij}^{+}(\omega) \ = \ \int \frac{dt}{2\pi} e^{i\omega t}\langle I_i(0)I_j(t)\rangle \ , \tag{3.6}$$

$$S_{ij}^{-}(\omega) \ = \ \int \frac{dt}{2\pi} e^{i\omega t}\langle I_i(t)I_j(0)\rangle \ . \tag{3.7}$$

Translation invariance relates these two correlators: $S^{-}_{ij}(\omega) = S^{+}_{ij}(-\omega)$, and furthermore $\langle I_i(\omega_1) I_j(\omega_2)\rangle = \delta(\omega_1 - \omega_2) S^{+}_{ij}(\omega_2)$, where $I_i(\omega)$ is the Fourier transform of $I_i(t)$. Note that only in the case of autocorrelation: $S^{+}_{ii}(\omega)$ ($S^{-}_{ii}(\omega)$) can be identified as an emission (absorption) rate from the mesoscopic device at positive frequencies. At this point, both integrals in Eq. (3.5) can be performed. The integration over t gives two contributions: one is a delta function, and the other gives products of principal parts, which cancel out. The charge fluctuations take the final form:

$$\begin{aligned}\langle x^2(0)\rangle \;=\; & \frac{\pi\alpha_1\alpha_2}{2\eta(2M)^2}\left[(N(\Omega)+1)(S^{+}_{12}(\Omega)+S^{+}_{21}(\Omega))\right. \\ & \left. -N(\Omega)(S^{-}_{12}(\Omega)+S^{-}_{21}(\Omega))\right] \;. \end{aligned} \tag{3.8}$$

To show that $\langle x^2(0)\rangle$ is real, we use the properties of the noise correlators: $[S^{\pm}_{ij}(\Omega)]^* = S^{\pm}_{ji}(\Omega)$, and the measured charge fluctuation reads:

$$\begin{aligned}\langle x^2(0)\rangle \;=\; & \frac{\pi\alpha_1\alpha_2}{\eta(2M)^2} Re\left[(N(\Omega)+1)S^{+}_{12}(\Omega)\right. \\ & \left. -N(\Omega)S^{-}_{12}(\Omega)\right] \;. \end{aligned} \tag{3.9}$$

This is a central result of this paper, which is illustrated below for a specific mesoscopic circuit. The LC measurement setup effectively measures the real part of the noise cross correlator. A similar result was mentioned in Ref. 22, although without justification. Note that the final result still depends on the adiabatic coupling parameter. In order to eliminate the dependence on η, the calculation can be generalized to a system with a distribution of oscillators, peaked around Ω. This is discussed in the appendix. The fact that the LC circuit has a finite line shape, has of course a physical origin: the LC circuit contains dissipative elements (due to both the finite conductivity of the wires and to the electronic environment which surround the circuit), but for simplicity we do not consider the detailed mechanism for dissipation here.

IV. MEASUREMENT WITH TWO LC CIRCUITS

Next, we examine the situation for using two separate circuits, with capacitors (C_1 and C_2) and two inductances (L_1 and L_2) with inductive coupling constants α_1 and α_2. The two LC circuits are placed next to the two outgoing arms of the three terminal mesoscopic device. The two capacitors is charging by the two inductances (Fig. 2).

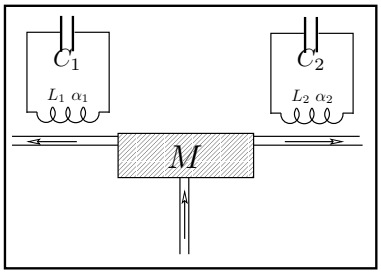

FIG. 2: Schematic description of the noise cross-correlation setup. M is the mesoscopic circuit to be measured, C_1 and C_2 are the two capacitors and there are two inductors with coupling constants α_1 and α_2 to the mesoscopic circuit.

The charges on each capacitor satisfy equations of motion similar to the previous calculation with a single circuit, where the "mass" $M_{1(2)} = L_{1(2)}$. The characteristic frequency of each LC circuit is $\Omega_{1(2)} = \sqrt{1/C_{1(2)}M_{1(2)}}$.

The second power of the capacitor two-charge correlator reads, in the interaction representation:

$$\langle x_1(0)x_2(0)\rangle = Tr[e^{-\beta(H_{0,1}+H_{0,2})}U^{-1}(0)x_1(0)x_2(0)U(0)] \ . \tag{4.1}$$

Note that unlike in the previous section, we do not provide a scenario here for finding an observable which corresponds to the measurement of the product of the two charges. We calculate perturbatively the n-th power of the charge, expanding the evolution term $(U(0))$ in powers of $H_{int,1(2)}$. Considering the average charge and the average charge square, one obtains:

$$\langle x_{1(2)}(0)\rangle \ = \ \langle x_{1(2)}(0)\rangle_1 + \langle x_{1(2)}(0)\rangle_3 + ... \ , \tag{4.2}$$

$$\langle x_1(0)x_2(0)\rangle \ = \ \langle x_1(0)x_2(0)\rangle_0 + \langle x_1(0)x_2(0)\rangle_2 + ... \ , \tag{4.3}$$

where the different orders in $H_{int,1(2)}$ are linked to the higher cumulants of the current: $\langle x_{1(2)}(0)\rangle_1$ contains information about the average current, the product $\langle x_1(0)x_2(0)\rangle_2$ about the current fluctuations, and $\langle x_{1(2)}(0)\rangle_3$ about the third moment, and so on.

The zero order contribution of the charge fluctuation $\langle x_1(0)x_2(0)\rangle_0$ becomes zero . The

first non-vanishing term, which depends on products of current operators is:

$$\begin{aligned}\langle x_1(0)x_2(0)\rangle_2 = \quad & \Big\langle \frac{1}{2}\int_{-\infty}^{0} dt_1 \int_{-\infty}^{t_1} dt_2 \\ & \times \Big[[x_1(0)x_2(0), \frac{-i}{\hbar M_1}p_1(t_1)\alpha_1 I_1(t_1) + \frac{-i}{\hbar M_2}p_2(t_1)\alpha_2 I_2(t_1)], \\ & \frac{-i}{\hbar M_1}p_1(t_2)\alpha_1 I_1(t_2) + \frac{-i}{\hbar M_2}p_2(t_2)\alpha_2 I_2(t_2)\Big]\Big\rangle \\ & - \frac{1}{2}\Big(\frac{-i}{\hbar}\Big)^2 \int_{-\infty}^{0} dt \Big\langle \Big(\frac{\alpha_1 I_1(t)}{M_1}\Big)^2 + \Big(\frac{\alpha_2 I_2(t)}{M_2}\Big)^2 \Big\rangle \langle x_1(0)x_2(0)\rangle \\ & - \langle x_1(0)x_2(0)\rangle \Big\langle \Big(\frac{\alpha_1 I_1(t)}{M_1}\Big)^2 + \Big(\frac{\alpha_2 I_2(t)}{M_2}\Big)^2 \Big\rangle \ . \end{aligned} \tag{4.4}$$

The calculation of the charge fluctuations gives four terms: two autocorrelation terms which correspond to the fluctuations due to a single inductor (in terms of α_1^2 or α_2^2), and two terms associated with the correlation between the two inductors, which are proportional to $\alpha_1\alpha_2$. In the two autocorrelation terms, we calculate the average of an odd number of creation and destruction operators for the each circuit. The autocorrelation is zero. The combination of current cross-correlators will be referred from now on as the measured cross-correlations.

Choosing a particular case where the two LC circuits have the same characteristic frequencies ($\Omega_1 = \Omega_2 = \Omega$), the charge fluctuations correspond to the result obtained in the presence of a single capacitor with two inductances (see Eq. 3.8). In practice, it is challenging to build two LC circuits with exactly the same characteristic frequency. The result of Eq. (3.8) for $\Omega_1 = \Omega_2$ has also appeared in Ref. [20]. For the case of different frequencies ($\Omega_1 \neq \Omega_2$), The charge fluctuations have a general form:

$$\begin{aligned}\langle x_1(0)x_2(0)\rangle = -\frac{\alpha_1\alpha_2}{2}\int_0^{+\infty} dt \Big\{ & \\ \times \ & \Big(\frac{e^{it(\Omega_1-\Omega_2)/2}}{\eta + i\frac{\Omega_1+\Omega_2}{2}} + \frac{e^{-it(\Omega_2+\Omega_1)/2}}{\eta + i\frac{-\Omega_1+\Omega_2}{2}}\Big)[(N(\Omega_2)+1)\langle I_1(t)I_2(0)\rangle - N(\Omega_2)\langle I_2(0)I_1(t)\rangle] \\ + \ & \Big(\frac{e^{it(\Omega_2+\Omega_1)/2}}{\eta + i\frac{\Omega_1-\Omega_2}{2}} + \frac{e^{it(\Omega_2-\Omega_1)/2}}{\eta - i\frac{\Omega_1+\Omega_2}{2}}\Big)[N(\Omega_2)\langle I_1(t)I_2(0)\rangle - (N(\Omega_2)+1)\langle I_2(0)I_1(t)\rangle] \\ + \ & \Big(\frac{e^{it(\Omega_2-\Omega_1)/2}}{\eta + i\frac{\Omega_1+\Omega_2}{2}} + \frac{e^{-it(\Omega_1+\Omega_2)/2}}{\eta + i\frac{\Omega_1-\Omega_2}{2}}\Big)[(N(\Omega_1)+1)\langle I_2(t)I_1(0)\rangle - N(\Omega_1)\langle I_1(0)I_2(t)\rangle] \\ + \ & \Big(\frac{e^{it(\Omega_1+\Omega_2)/2}}{\eta + i\frac{-\Omega_1+\Omega_2}{2}} + \frac{e^{it(\Omega_1-\Omega_2)/2}}{\eta + i\frac{-\Omega_1-\Omega_2}{2}}\Big)[N(\Omega_1)\langle I_2(t)I_1(0)\rangle - (N(\Omega_1)+1)\langle I_1(0)I_2(t)\rangle]\Big\} \ , \end{aligned} \tag{4.5}$$

which result in delta function contributions, as well as (unwanted) principal parts: strictly speaking the charge fluctuations do not simplify. However, a practical measurement always

involves some bandwidth averaging, which could possibly lead to a result close to that of the case $\Omega_1 = \Omega_2$.

Furthermore, the use of two separate capacitors should also consider the multiplication process of the two charge operators. Multiplication of two signals involves adding and subtracting the two signals, then squaring and subtracting. In these steps of the measurement, the noise from the amplifiers will be detrimental in the same manner as in the case of a single LC circuit.

V. APPLICATION TO A THREE TERMINAL NORMAL CONDUCTOR

Next, we consider noise measurement with the single capacitor and two inductances circuit initially proposed. It is tested on a system of three terminals (Fig 3), a so called "Y junction", electrons are injected from terminal 1, which has a higher chemical potential than terminals 2 and 3. The noise cross–correlations are measured. This corresponds to the setup where a fermionic analog of Hanbury–Brown and Twiss type experiments[23] was proposed[7] and measured[15]. Without loss of generality, one considers that the three bias voltages, $\mu_{ij} = \mu_i - \mu_j$, $(i, j = 1, 2, 3)$, are chosen such that $\mu_{13} > \mu_{12}, \mu_{23}$.

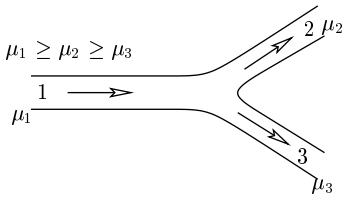

FIG. 3: A system with three terminals (Y junction) with chemical potentials μ_1, μ_2 and μ_3 with $\mu_1 \geq \mu_2 \geq \mu_3$.

Using scattering theory, one can readily obtain the general expression for the non-symmetrized finite frequency noise[21]:

$$\begin{aligned} S^{+}_{\alpha\beta}(\omega) \;=\; \frac{e^2}{2\pi\hbar} \sum_{\gamma\delta} \int dE \; & (\delta_{\alpha\gamma}\delta_{\alpha\delta} - s^{\dagger}_{\alpha\gamma}(E) s_{\alpha\delta}(E - \hbar\omega)) \\ & \times (\delta_{\beta\delta}\delta_{\beta\gamma} - s^{\dagger}_{\beta\delta}(E) s_{\beta\gamma}(E - \hbar\omega)) \\ & \times f_{\gamma}(E)(1 - f_{\delta}(E - \hbar\omega)) \;, \end{aligned} \tag{5.1}$$

where Greek letters represent the terminals and $s_{\alpha,\beta}$ is the scattering amplitude for electrons incoming from β and ending in α. $f_\gamma(E)$ is the Fermi-Dirac distribution function associated

with terminal γ whose chemical potential is μ_γ. In what follows we assume that the temperature is much smaller than the applied biases. One also neglects the energy dependence of the scattering matrix over the energy ranges specified by the voltages biases μ_{ij}. Furthermore, Eq. (5.1) neglects $\pm 2k_F$ oscillating terms in the noise fluctuations spectrum: this assumes that the region over which current is measured is much larger than the Fermi wave length, $l \gg \lambda_F$.

For $\mu_{23} < \mu_{12}$ and at negative frequencies, cross-correlations between terminals 2 and 3 yield:

$$S_{23}^+(\omega) \;=\; S_{32}^+(\omega) = -\frac{e^2}{2\pi}\omega(T_{21}T_{13} - (2 - R_2 - R_3)T_{23}) \\ -\frac{e^2}{2\pi\hbar}\begin{cases} (-\hbar\omega)(2T_{13}R_3 + 2T_{12}R_2 + 2T_{23}R_2) & \text{if } \hbar\omega < -\mu_{13} \\ T_{13}R_3(\mu_{13} - \hbar\omega) - \hbar\omega(2T_{12}R_2 + 2T_{23}R_2) & \text{if } -\mu_{13} < \hbar\omega < -\mu_{12} \\ T_{13}R_3(\mu_{13} - \hbar\omega) + T_{12}R_2(\mu_{12} - \hbar\omega) - \hbar\omega(2T_{23}R_2) & \text{if } -\mu_{12} < \hbar\omega < -\mu_{23} \\ T_{23}R_2(\mu_{23} - \hbar\omega) + T_{13}R_3(\mu_{13} - \hbar\omega) + T_{12}R_2(\mu_{12} - \hbar\omega) & \text{if } -\mu_{23} < \hbar\omega < 0 \end{cases} \tag{5.2}$$

while for positive frequencies:

$$S_{23}^+(\omega) \;=\; S_{32}^+(\omega) = -\frac{e^2}{2\pi\hbar}\begin{cases} T_{23}R_2(\mu_{23} - \hbar\omega) + T_{13}R_3(\mu_{13} - \hbar\omega) + T_{12}R_2(\mu_{12} - \hbar\omega) & \text{if } 0 < \hbar\omega < \mu_{23} \\ T_{13}R_3(\mu_{13} - \hbar\omega) + T_{12}R_2(\mu_{12} - \hbar\omega) & \text{if } \mu_{23} < \hbar\omega < \mu_{12} \\ T_{13}R_3(\mu_{13} - \hbar\omega) & \text{if } \mu_{12} < \hbar\omega < \mu_{13} \\ 0 & \text{if } \mu_{13} < \hbar\omega \end{cases} \tag{5.3}$$

where $R_\alpha = s^\dagger_{\alpha,\alpha}s_{\alpha,\alpha}$ is the reflection probability from lead α and $T_{\alpha\beta} = s^\dagger_{\alpha,\beta}s_{\alpha,\beta} = T_{\beta\alpha}$ is the transmission probability from α to β.

As expected, the frequency dependence is given by a set of continuous straight lines with singular derivatives. At zero frequency, the non-symmetrized cross-correlations are:

$$S_{23}^+(\omega = 0) \;=\; -\frac{e^2}{2\pi\hbar}(T_{23}R_2\mu_{23} + T_{13}R_3\mu_{13} \\ + T_{12}R_2\mu_{12}) \; . \tag{5.4}$$

The cross-correlations are negative regardless of bias voltage and transmission of the sample: one recovers the result of Ref. 7.

On the other hand, the symmetrized finite frequency cross-correlations are defined by:

$$S_{23}^S(\omega) = \int d\omega e^{i\omega t}\langle \Delta I_2(t)\Delta I_3(0) + \Delta I_3(0)\Delta I_2(t)\rangle \; , \tag{5.5}$$

with $\Delta I(t) = I(t) - \langle I(t)\rangle$. From Ref. 2, when $\mu_{23} < \mu_{12}$ and at zero temperature, one obtains:

$$S_{23}^S(\omega) = -\frac{e^2}{2\pi}|\omega|(T_{21}T_{13} - (2 - R_2 - R_3)T_{23}) - \frac{e^2}{2\pi\hbar}\begin{cases} +T_{23}R_2\mu_{23} + T_{13}R_3\mu_{13} + T_{12}R_2\mu_{12} & \text{if } |\hbar\omega| < \mu_{23} \\ \hbar|\omega|(T_{23}R_2) + T_{13}R_3\mu_{13} + T_{12}R_2\mu_{12} & \text{if } \mu_{23} < |\hbar\omega| < \mu_{12} \\ \hbar|\omega|(T_{12}R_2 + T_{23}R_2) + T_{13}R_3\mu_{13} & \text{if } \mu_{12} < |\hbar\omega| < \mu_{13} \\ \hbar|\omega|(T_{13}R_3 + T_{12}R_2 + T_{23}R_2) & \text{if } \mu_{13} < |\hbar\omega| \end{cases} \tag{5.6}$$

The frequency dependence of $S_{23}^S(\omega)$ is symmetric in ω. The non-symmetrized cross-correlations, given by Eqs. (5.2) and (5.3), coincides with the symmetrized cross-correlations at $\omega = 0$, as illustrated in Fig. 4. The non-symmetrized cross-correlations behavior is quite different from the symmetrized cross-correlations, although the locations of their singularities are the same. The symmetrized and non-symmetrized cross-correlations are both negative. The non-symmetrized cross-correlations are monotonously increasing and equal to zero for $\hbar\omega > \mu_{13}$.

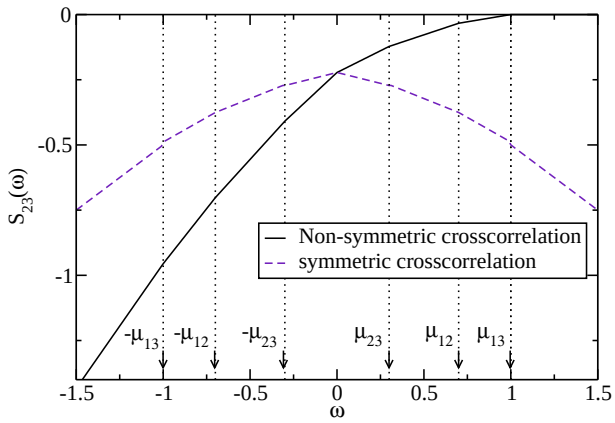

FIG. 4: Comparison between non-symmetrized and symmetrized cross-correlations as a function of frequency for $\mu_{12} > \mu_{23}$, in units of $e^2\mu_{13}/2\pi\hbar$. Singularities occur at $\hbar\omega = 0$, $\pm\mu_{23}$, $\pm\mu_{12}$, $\pm\mu_{13}$. The curves are plotted for $\mu_{12} = 0.7\mu_{13}$ and $\mu_{23} = 0.3\mu_{13}$.

We now consider the measured cross-correlations, given by Eq. (3.8), as a function of temperature of the measurement circuit. Because of the symmetry of the transmission probabilities, we have in this case $S_{23}^{\pm}(\omega) = S_{32}^{\pm}(\omega)$ [9, 10]. With the above symmetry consideration, the charge fluctuations resemble the formula for auto-correlation noise:

$$\langle x^2(0)\rangle = \frac{\alpha_1\alpha_2\pi}{\eta(2M)^2}[S_{23}^{+}(\omega) + \Delta S_{23}(\omega)N(\omega)] \ . \tag{5.7}$$

Note that it is the difference of the two non–symmetrized correlators $\Delta S_{23}(\omega) = S^+_{23}(\omega) - S^+_{23}(-\omega)$ which is multiplied by the Bose distribution $N(\omega)$:

$$\Delta S_{23}(\omega) = -\frac{e^2}{2\pi}\omega\Big(T_{21}T_{13} - (2 - R_2 - R_3)T_{23} \\ -2T_{13}R_3 - 2T_{12}R_2 - 2T_{23}R_2\Big) , \tag{5.8}$$

i.e., it is linear with frequency with a positive slope, and does not have any singularities.

Taking $\mu_2 = \mu_3$ for simplicity, the measured cross-correlations are plotted in Fig. 5.

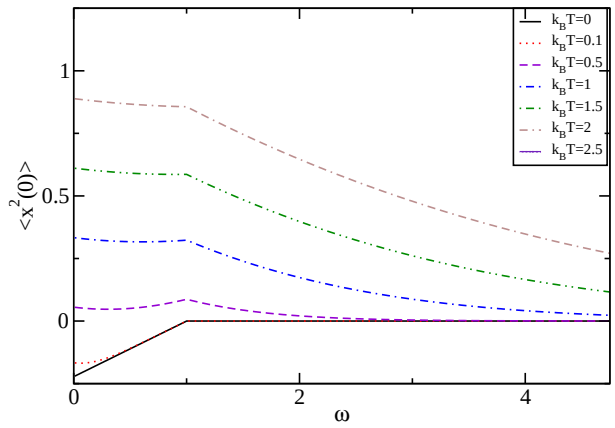

FIG. 5: Measured charge fluctuations as a function of frequency for different temperatures k_BT, measured in units of μ_{13}. The frequency and the biases are in units of μ_{13}.

For temperatures such that $k_BT \gtrsim \mu_{13}$, the Bose distribution is large, $N(\omega) \sim k_BT/\hbar\omega \gg 1$. $\Delta S_{23}(\omega)N(\omega)$ is thus larger than $|S^+_{23}(\omega)|$. The effect of the increasing temperature is to change the sign of the charge fluctuations which becomes positive. This may seem change given the fact that one is computing the fluctuations of charge at the plates of a capacitor: recall that our measurement implicitly assumes two experiments with different wiring, whose results are subtracted one from another. The main message of Fig. 5 is that the sign of the measured correlation can be misleading if the temperature of the measuring device is too large: one can observe positive cross-correlations in a normal fermionic fork although this is a system where anti-bunching is expected. For $\omega \geq \mu_{13}$, the measured noise equals $\Delta S_{23}(\omega)N(\omega)$, while for $\omega < \mu_{13}$, $S^+_{23}(\omega)$ lowers $\Delta S_{23}(\omega)N(\omega)$. At all temperatures, the measured charge fluctuations have a clear singularity at $\hbar\omega = \mu_{13}$: we are not taking into account the thermal effects in the mesoscopic circuit itself.

At low temperature, $k_BT \ll \mu_{13}$, and low frequency, $\omega \ll \mu_{13}$, $\Delta S_{23}(\omega)N(\omega)$ is smaller

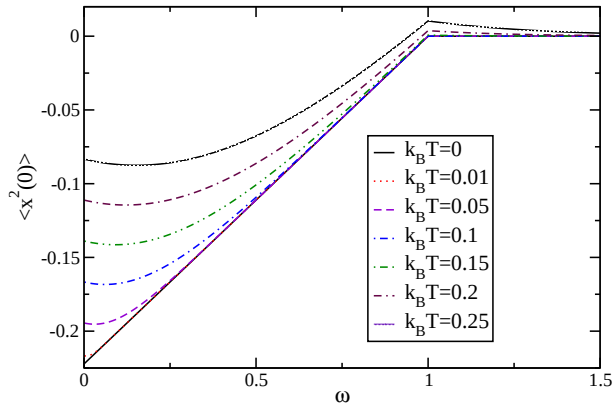

FIG. 6: Same as Fig. 5, for a smaller frequency range and at lower temperatures (in units of μ_{13}).

than $|S_{23}^{+}(\omega)|$ and the measured signal remains negative (see Fig. 6). When the temperature goes to zero, the measured charge fluctuations equal $S_{23}^{+}(\omega)$.

For completeness, the case where the voltage biases satisfy $\mu_{13} > \mu_{12} > \mu_{23} > 0$ is discussed. The fact that terminals 2 and 3 have different chemical potential will lower the contribution of $S_{23}^{+}(\omega)$ to $\Delta S_{23}(\omega)N(\omega)$, and increase the amplitude of charge fluctuations. At low temperature, the charge fluctuations stay negatives and singularities are present at frequencies equal to μ_{23}, μ_{12}, μ_{13}. When the temperature becomes larger than the bias voltages, the charge fluctuations become positive. However, when the temperature goes to zero, the charge fluctuations become equal to $S_{23}^{+}(\omega)$. When the difference between the chemical potentials of terminals 2 and 3 increases the effect of temperature is more important at small temperature the amplitude is bigger regardless of the effect of $S_{23}^{+}(\omega)$ is less important for large temperatures.

VI. WHEN ARE FINITE FREQUENCY CROSS-CORRELATIONS NOISE USEFUL ?

When probing quantum non-locality with a source of electrons (for instance a S–wave superconductor or any other source of electrons) with the help of Bell inequalities[24], one is confronted with the fact that particle number correlators must be converted into noise correlators. The particle number operator reads:

$$N_\alpha(\tau) = \int_0^\tau I_\alpha(t')dt' = \langle N_\alpha(\tau)\rangle + \delta N_\alpha(\tau) \ , \tag{6.1}$$

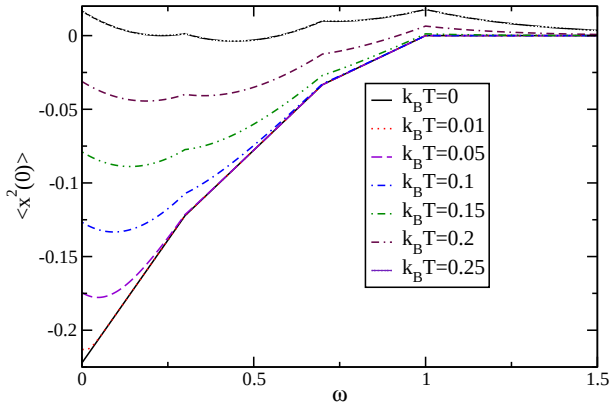

FIG. 7: Same as Fig. 5, for a smaller frequency range, and at lower temperatures. $\mu_{12} = 0.7\mu_{13}$, $\mu_{23} = 0.3\mu_{13}$ have been chosen.

where $I_\alpha(t)$ is the current operator in lead α. The irreducible particle number correlator is expressed in terms of the finite frequency shot noise power:

$$\langle \delta N_\alpha(\tau)\delta N_\beta(\tau)\rangle = (1/2\pi)\int_{-\infty}^{\infty} d\omega S_{\alpha,\beta}(\omega) 4\sin^2(\omega\tau/2)/\omega^2 \ . \tag{6.2}$$

It is therefore only in the limit of relatively "large" acquisition times that the Bell inequality can be cast in terms of zero frequency correlations only[24, 25], thus the need in general to measure in general finite frequency noise correlations. This is implicit in the work of Ref. 26, where entanglement occurs with a normal source of electrons, provided that short time dynamics can be analyzed. Ref. 24 missed this subtlety concerning normal electron sources.

Another situation of interest for finite frequency cross-correlations noise deals with the detection of anomalous (non-integer charges) in carbon nanotube. A Hanbury–Brown and Twiss experiment has been proposed where an STM tip injects electron in the bulk of the nanotube and cross-correlations noise are measured at the extremities of the nanotube[18, 27]. In Ref. 27, the case of an infinite nanotube has been considered. Schottky-like relations for the zero-frequency Fourier transforms of the auto-correlation noise and the cross-correlations noise were derived within the Tomonaga-Luttinger model:

$$S_{auto}(\omega = 0) = \frac{1 + (K_{c+})^2}{2} e|\langle I(x)\rangle| \ , \tag{6.3}$$

$$S_{cross}(\omega = 0) = \frac{1 - (K_{c+})^2}{2} e|\langle I(x)\rangle| \ , \tag{6.4}$$

where $\langle I(x)\rangle$ is the charge current through the nanotube and K_{c+} is the Luttinger liquid interaction parameter. S_{auto} is the term of auto-correlations and S_{cross} is the cross-correlations term. However, in the presence of electrical contacts at the extremities of the nanotube, the zero-frequency Fourier transforms for noise and cross-correlations lose their K_{c+}-dependence: at order 2 in the perturbative expansion with the tunneling amplitude from the tip to the nanotube, they reduce to $S_{auto}(\omega = 0) = e|\langle I(x)\rangle|$ and $S_{cross}(\omega = 0) = 0$. It has been shown in Ref. [18], that one has to consider finite frequency Fourier transform in order to recovered non zero cross-correlations and coulomb interactions effects in such a system.

VII. CONCLUSION

In summary, we have shown that the cross-correlations noise of a mesoscopic circuit can be measured by coupling the latter to a resonant circuit which is composed of two inductances and a capacitor. Each inductance is attached to the arms where correlations are measured. As in Ref. [9], the proposed noise measurement is made by monitoring the charge fluctuations on the capacitor. Two distinct measurements, with different wiring of the circuit, are necessary to isolate the cross-correlations noise.

Granted, we have not described the experimental apparatus which is needed to convert the signal into classical information, i.e. the amplification scheme: this goes beyond the scope of the present paper, which goal is to convey that information about cross-correlations noise can be converted into a charge signal on a capacitor. A general approach for analyzing the quantum behavior of electronic circuitry has been proposed [28], allowing to treat both nonlinear and dissipative elements, hence useful for signal conversion. The transition from mesoscopic to macroscopic quantum transport has been addressed in the context of scattering theory [29]. Note that in our analysis of the setup, the variable $\dot{x}$ denotes the current flowing in the capacitor's circuit. It is assumed to be a constant current in space. This description may be inappropriate at high frequencies, setting some upper limit to the frequencies we want to probe.

Note that the quality of the diagnosis of cross-correlations presented in this work depends, to a large extent, on how the mesoscopic circuit is perturbed when one switches from one wiring configuration to the other. Indeed, it is necessary to minimize the changes in configuration (the values of α_1 and α_2) of the circuit which occurs between the two measurements. Here one could assume ideally that the inductances are built "on-chip" with the

mesoscopic circuit, or with the wires connected to it, which is a challenge in practice: small inductors working at high frequencies ($\omega = 100GHz$) may be difficult to achieve. While it may be more realistic to couple the two circuits away from the mesoscopic device, on chip inductances of small scale are nevertheless used in qbit circuitry [30]. Moreover, the wires of the measurement circuit are assumed to have a low impedance compared to that of the mesoscopic sample: within these working conditions the change of wiring does not affect significantly the inductive couplings, and the measurement will be reliable.

As a first necessary application of this measurement scheme, we considered a three terminal normal metal conductor, which is known to exhibit negative noise correlations at zero frequency. The symmetrized noise differs strongly from the non-symmetrized noise and the measured noise. For a mesoscopic circuit at zero temperature, the non-symmetrized noise contains singularities at frequencies corresponding to the chemical potential differences. However, when considering the measured noise, care must be taken to work with a detector circuit whose temperature is below these relevant biases. In this case the singularities in the derivative can still be detected, and upon increasing slowly the temperature, the measured noise deviates from the non-symmetrized noise. This provides a condition for the observation of negative noise correlations – electron anti-bunching – in such three terminal devices. Because of the above mentioned temperature effects of the device, the amplifiers needed for signal conversion would need to be cooled down in order to avoid such problems.

The present analysis can be extended to study the measured noise correlations in other mesoscopic devices, in particular three terminal structures where electrons are injected in one lead from a superconductor[31]. Finite frequency noise correlations in this case contain information of the time dynamics of the two electrons subject to crossed-Andreev transport.

APPENDIX A

We discuss the case where the resonant LC circuit has a finite line shape. For a distribution of oscillators, the charge operator now takes the form:

$$x(t) = \sum_{\omega} x_{\omega}(t) = \sum_{\omega} \sqrt{\hbar/2M\omega}(a_{\omega}e^{-i\omega t} + a_{\omega}^{\dagger}e^{i\omega t}) \ , \tag{A1}$$

where the interaction coupling, $-\alpha Ip/M$, becomes $-I\sum_{\omega}\alpha_{\omega}p_{\omega}/M$.

These expressions are substituted in the interlocked commutators Eq. (2.9), which now contains a sum over 4 frequencies ω_1, ω_2, ω_3 and ω_4. Because of time integrations, delta

functions appear and give equalities between the frequencies. We are left with two summations:

$$\begin{aligned}
&\left\langle \left[[x^2(0), p(t_1) I_i(t_1)], p_(t_2) I_j(t_2) \right] \right\rangle = \\
&\quad \sum_{\omega_1, \omega_2} \hbar^2 \cos(\omega_1 t_1) \\
&\quad \times \Big[\langle I_i(t_1) I_j(t_2) \rangle (N_{\omega_2} e^{-i\omega_2 t_2} - (N_{\omega_2}+1) e^{i\omega_2 t_2}) \\
&\quad - \langle I_j(t_2) I_i(t_1) \rangle ((N_{\omega_2}+1) e^{-i\omega_2 t_2} - N_{\omega_2} e^{i\omega_2 t_2}) \Big] \ . \qquad \text{(A2)}
\end{aligned}$$

We substitute this expression in the charge fluctuations and proceed with the change of variable, we make use of the time translational invariance: $t = t_1 - t_2$ and $T = t_1 + t_2$ and $\langle I_i(t) I_j(0) \rangle = \langle I_i(0) I_j(-t) \rangle$. Making use of the definitions of Eqs. (3.6) and (3.7), the integral over T leads to two contributions:

$$\begin{aligned}
K_1 &= \int_{-\infty}^{0} dT e^{i(\omega_1+\omega_2)t/2} e^{\eta T + i(\omega_1-\omega_2) sign(t) T/2} \\
&= \frac{e^{i(\omega_1+\omega_2)t/2}}{\eta + i(\omega_1-\omega_2) sign(t)/2} \ , \qquad \text{(A3)} \\
K_2 &= -\int_{-\infty}^{0} dT e^{i(-\omega_1+\omega_2)t/2} e^{\eta T - i(\omega_1+\omega_2) sign(t) T/2} \\
&= -\frac{e^{i(-\omega_1+\omega_2)t/2}}{\eta - i(\omega_1+\omega_2) sign(t)/2} \ . \qquad \text{(A4)}
\end{aligned}$$

The line shape $L(\omega - \Omega)$, which is sharply peak around the resonant circuit frequency Ω, is introduced when converting discrete sums over frequencies into integrals. The integral over t is performed subsequently.

The denominators of K_1 and K_2 yield a real part which are a principal part and an imaginary part which are a Dirac delta function. We obtain four contributions for the charge fluctuations:

$$\langle x^2(0) \rangle = A_1 + A_2 + A_3 + A_4 \ , \qquad \text{(A5)}$$

where

$$A_1 = 4\pi^2 \int d\omega L^2(\omega-\Omega)\frac{\alpha_1\alpha_2}{(2M)^2} \times Re\left[(N_\omega+1)S_{12}^+(\omega) - N_\omega S_{12}^-(\omega)\right] \ , \quad \text{(A6)}$$

$$A_2 = -2\int d\omega_1 d\omega_2 d\omega_3 L(\omega_1-\Omega)L(\omega_2-\Omega)\frac{\alpha_1\alpha_2}{(2M)^2} \times \mathcal{P}\Big(((\omega_1+\omega_2)/2-\omega_3)^{-1}\Big)\mathcal{P}\Big(2/(\omega_1-\omega_2)\Big) \times Re\left[(N_{\omega_2}+1)S_{12}^+(\omega_3) - N_{\omega_2}S_{12}^-(\omega_3)\right] \ , \quad \text{(A7)}$$

$$A_3 = 4\pi^2 \int d\omega L(\omega-\Omega)L(-\omega-\Omega)\frac{\alpha_1\alpha_2}{(2M)^2} \times Re\left[(N_\omega+1)S_{12}^+(-\omega) - N_\omega S_{12}^-(-\omega)\right] \ , \quad \text{(A8)}$$

$$A_4 = -2\int d\omega_1 d\omega_2 d\omega_3 L(\omega_1-\Omega)L(\omega_2-\Omega)\frac{\alpha_1\alpha_2}{(2M)^2} \times \mathcal{P}\Big(((\omega_1-\omega_2)/2-\omega_3)^{-1}\Big)\mathcal{P}\Big(2/(\omega_1+\omega_2)\Big) \times Re\left[(N_{\omega_2}+1)S_{12}^+(\omega_3) - N_{\omega_2}S_{12}^-(\omega_3)\right] \ , \quad \text{(A9)}$$

where the function $\mathcal{P}$ gives the principal part. The contribution which dominates is the contribution where the two line shape functions $L(\omega-\Omega)$ are peaked at the same frequency, i.e., Eq (A6). The quantity η which appears in the single oscillator model thus corresponds physically to the width of the line shape, as expected.

---

[1] S.R. Eric Yang, Solid State Commun. **81**, 375 (1992).

[2] Y.M. Blanter and M. Büttiker, Phys. Rep. **336**, 1 (2000).

[3] B. Tzauzettel and H. Grabert, Phys. Rev. B **67**, 245101 (2003).

[4] Y. Levinson and Y. Imry, in Proc. of the NATO ASI "Mesoscope 99" in Ankara, Antalya, Kluver 1999.

[5] J. Torrès, T. Martin, and G. Lesovik Phys. Rev. B **63**, 134517 (2001).

[6] C. Chamon, D. E. Freed, and X. G. Wen, Phys. Rev. B **53**, 4033 (1996).

[7] T. Martin and R. Landauer, Phys. Rev. B **45**, 1742 (1992); M. Büttiker, Phys. Rev. B **45**, 3807 (1992).

[8] R. J. Schoelkopf, P. J. Burke, A. A. Kozhevnikov, D. E. Prober, and M. J. Rooks, Phys. Rev. Lett. **78**, 3370 (1997).

[9] G. B. Lesovik and R. Loosen, Pis'ma Zh. Éksp. Teor. Fiz. **65**, 280 (1997) [JETP Lett. **65**, 295, (1997)].

[10] Y. Gavish, I. Imry, and Y. Levinson, Phys. Rev. B **62**, 10637 (2000).

[11] R. Aguado and L. Kouwenhoven, Phys. Rev. Lett. **84**, 1986 (2000).

[12] R. Deblock, E. Onac, L. Gurevich, and L. P. Kouvenhoven, Science **301**, 203 (2003).

[13] P.-M. Billangeon, F.Pierre, H. Bouchiat, and R. Deblock, cond-mat/0508676.

[14] J. Gabelli, L.-H. Reydellet, G. Feve, J.-M. Berroir, B. Plaçais, P. Roche, and D. C. Glattli, Phys. Rev. Lett. **93**, 056801 (2004).

[15] M. Henny, S. Oberholzer, C. Strunk, T. Heinzel, K. Ensslin, M. Holland, and C. Schönenberger, Science **284**, 296 (1999); W. D. Oliver, J. Kim, R. C. Liu, and Y. Yamamoto, Science **284**, 299 (1999).

[16] G. B. Lesovik, T. Martin, and G. Blatter, Eur. Phys. J. B. **24**, 287 (2001).

[17] P. Recher, E.V. Sukhorukov, and D. Loss, Phys. Rev. B **63**, 165314 (2001).

[18] A. V. Lebedev, A. Crépieux, and T. Martin, Phys. Rev. B **71**, 075416 (2005).

[19] Y. Gavish, Y. Levinson, and Y. Imry, Phys. Rev. Lett. **87**, 216807 (2001).

[20] Y. Gavish, PhD Thesis (2003).

[21] T. Martin in Les Houches Summer School session LXXXI, edited by E. Akkermans, H. Bouchiat, S. Gueron, and G. Montambaux (Springer, 2005).

[22] G. B. Lesovik, A. V. Lebedev, and G. Blatter, Phys. Rev. B **71**, 125313 (2005).

[23] R. Hanbury-Brown and R. Q. Twiss, Nature **177**, 27 (1956).

[24] N. Chtchelkatchev, G. Blatter, G. Lesovik, and T. Martin, Phys. Rev. B **66**, 161320 (2002).

[25] C. W. J. Beenakker, C. Emary, M. Kindermann, and J. L. van Velsen, Phys. Rev. Lett **91**, 147901 (2003); C. W. J. Beenakker and M. Kindermann, Phys. Rev. Lett **92**, 056801 (2004); P. Samuelsson, E. V. Sukhorukov, and M. Buttiker, Phys. Rev. Lett **91**, 157002 (2003); P. Samuelsson, E.V. Sukhorukov, and M. Büttiker Phys. Rev. Lett. **92**, 026805 (2004).

[26] A. V. Lebedev, G. B. Lesovik, and G. Blatter, Phys. Rev. B **71**, 045306 (2005).

[27] A. Crépieux, R. Guyon, P. Devillard, and T. Martin, Phys. Rev. B **67**, 205408 (2003).

[28] B. Yurke and J.S. Denker, Phys. Rev. A **29**, 1419 (1984).

[29] R.C. Liu and Y. Yamamoto, Phys. Rev. B **50**, 17411 (1994).

[30] T. Duty et al., Phys. Rev. Lett. **95**, 206807 (2005).

[31] J. Torrès and T. Martin, European Phys. J. B **12**, 319 (1999).